

Lifetime of virion-containing droplets diffusing and evaporating in air

Roland R. Netz, Physics Department, Freie Universität Berlin, 14195 Berlin, Germany

Abstract: *For accurate estimates of the falling time of water droplets in air, evaporation must be taken into account, which involves different effects. For droplet radii in the range $100\text{ nm} < R < 60\text{ }\mu\text{m}$, evaporation can be described by the stagnant-flow approximation and is diffusion limited. For droplets smaller than $R=100\text{ nm}$, evaporation becomes rate limited. For radii larger than $60\text{ }\mu\text{m}$, the Stokes description of the air-flow profile around the droplet becomes invalid and non-linear hydrodynamic effects produce a flow boundary layer. Also, the air flow accelerates water diffusion away from the droplet, which can be described by a concentration boundary layer. Thus, for droplets larger than $R=60\text{ }\mu\text{m}$, the evaporation process is described by a double-boundary layer scenario, but stays diffusion-limited. Analytical equations are presented for the droplet evaporation rate and the time-dependent droplet size including the significant droplet cooling due to evaporation. For an initial height of 2 meters and a relative humidity $RH=1/2$, droplets with radii below $49\text{ }\mu\text{m}$ shrink rapidly down to a minimal radius due to evaporation during their descent to the floor and remain floating in air for a long time. In the presence of non-volatile solutes in the droplets, the final droplet radius and thus the time droplets remain floating in air, depends on the initial solute fraction. Low relative humidity, as encountered inside buildings in winter and in airliners, speeds up evaporation and thus keeps initially larger droplets suspended in air. Recent time-resolved laser light-scattering experiments show that a large number of droplets of oral fluid are emitted into the air while speaking (1). For a quantitative assessment of the lifetime of oral fluid droplets, it is important to measure the time-resolved size distribution of emitted droplets while speaking and coughing and their virion content.*

This note addresses the problem of diffusing liquid droplets in the presence of gravitational force, evaporation, and an absorbing boundary condition at the ground. This is a classical problem that has been treated in many experimental and theoretical previous works (2; 3; 4; 5; 6; 7; 8; 9; 10; 11) and is covered in textbooks (12). Many previous works considered raindrops, for which the relevant radii range from $100\text{ }\mu\text{m}$ to millimeters. Duguid studied droplet sizes produced by humans sneezing, coughing and speaking by microscopy analysis of marks left on slides and found droplet radii between 1 and $500\text{ }\mu\text{m}$ (4). In fact, 95% of all particles had radii below $50\text{ }\mu\text{m}$, and most final droplet radii were around $5\text{ }\mu\text{m}$. Later studies basically confirmed these results and showed that additionally, many droplets are produced in the nanometer radius range during coughing and speaking (13; 14; 15; 16; 17; 18). In one study a multimodal droplet size distribution was found and rationalized in terms of distinct physiological production loci (19). It was shown that the number of droplets produced while speaking depends among other factors on the voice loudness (20) and that the droplet production while exhaling is the product of complex fluid fragmentation processes (21). Recent time-resolved sensitive laser-light scattering measurements showed that far more droplets are produced than could be previously measured (1), which demonstrates that the measured droplet radius distribution depends on the size sensitivity of the measurement technique used and also on the time the droplets spend in air before measurement. In the present work, evaporation effects for droplets with radii in the range from nm to few hundreds μm are considered, which is the range most relevant for airborne virus infection

(22; 23; 24; 25). The calculations include the interplay of various relevant physical effects: i) the maximal evaporation reaction rate at the droplet surface, ii) concentration-boundary as well as flow-boundary layers, iii) droplet cooling due to the large evaporation enthalpy of water, iv) the water vapor pressure reduction due to the presence of non-volatile solutes in the droplet. Analytical expressions for the evaporation rate and the time-dependent radius are derived in all relevant radius regimes. When neglecting evaporation effects, a droplet with a radius of 5 μm that is released at an initial height of 2 meters stays suspended in air for 11 minutes before it falls to the ground, which is a sufficiently long time to be relevant for estimates of the infection probability by aerosols. By an exact calculation of the falling time distribution, it is shown that the droplet falling time is accurately estimated by its mean, which in turn is described by the mean speed a droplet acquires due to the gravitational force with resistance from Stokes friction: positional fluctuation effects are negligible for droplet radii above 10 nm. Evaporation effects are easily treated on the level of the diffusion equation in the stagnant approximation, i.e. neglecting the flow field around the droplet, and in the diffusion-limited evaporation regime. This approximation is only accurate for droplet radii in the range $100 \text{ nm} < R < 60 \mu\text{m}$. For radii larger than $60 \mu\text{m}$, the flow around the droplet speeds up the evaporation process and at the same time becomes non-Stokesian due to non-linear hydrodynamics effects, which can be treated analytically by double-boundary-layer theory including concentration and flow boundary layers. Whether the concentration boundary layer or the flow boundary is dominant, depends on the relative air humidity. Evaporation cooling is important and reduces the droplet surface temperature by about 9 Kelvin at a relative humidity of $\text{RH}=1/2$, which slows down evaporation. For radii smaller than 100 nm, the evaporation at the droplet-air interface becomes reaction-rate limited. For these small droplets, the evaporation rate is not limited by the speed with which water molecules diffuse away from the droplet surface, but rather by the rate at which water evaporates from the liquid surface.

Including evaporation, the falling time of a dried droplet is determined by the final droplet radius, which depends primarily on the solute concentration. Saliva contains approximately 99.5 % water and thus a solute weight fraction of $1/200$, meaning that the droplet radius can maximally decrease by a factor of $200^{1/3} = 6$. If saliva would completely dry out, a droplet with an initial radius of about $R = 30 \mu\text{m}$ shrinks at a relative humidity of $\text{RH}=0.5$ down to a radius of $R = 5 \mu\text{m}$ in about 5.4 s and then stays floating in air for about 11 minutes. The water vapor-pressure reduction due to the presence of solutes inside the droplet change this estimate only slightly. As a result of evaporation, the solute concentration has increased by a factor of 200. Residual hydration water that stays in the final droplet changes this estimate only slightly. In addition to the finite solute concentration, a kinetically important factor is shown to be the diffusion speed of water z_0 within the droplet, which becomes a limiting factor for the evaporation rate for droplet radii above $R= 100 \mu\text{m}$.

It is useful to first recapitulate a few well-known basic equations in the absence of evaporation. By balancing the gravitational force, proportional to the acceleration g , that acts on a droplet with radius R and density ρ , with the Stokes friction, the mean falling time (see Appendix A) is

$$\tau_a = \frac{k_B T z_0}{D_R m g} = \frac{9 \eta z_0}{2 \rho R^2 g} = \varphi \frac{z_0}{R^2} \quad , \quad (1)$$

where the Stokes expression is used for the droplet diffusion constant $D_R = k_B T / (6\pi\eta R)$, droplet mass is given by $m = 4\pi R^3 \rho / 3$, and values for the viscosity of air η , water density ρ , thermal energy $k_B T$, and the gravitational constant g are given in Table I. The numerical prefactor in Eq. (1) turns out to be $\phi = 0.85 \times 10^{-8} \text{ m s}$. For a droplet placed initially at a height of $z_0 = 2 \text{ m}$ and droplet radii $R = 100 \text{ }\mu\text{m}$, $R = 10 \text{ }\mu\text{m}$, **$R = 5 \text{ }\mu\text{m}$** , $R = 1 \text{ }\mu\text{m}$, 100 nm , the falling times are $\tau_a = 1.7 \text{ s}$, $\tau_a = 170 \text{ s}$, **$\tau_a = 680 \text{ s} = 11 \text{ minutes}$** , $\tau_a = 17,000 \text{ s} = 5 \text{ hours}$, $\tau_a = 1.7 \times 10^6 \text{ s} = 20 \text{ days}$. The droplet radius $R = 5 \text{ }\mu\text{m}$ with a falling time of 11 minutes is typically defined as a threshold radius below which the falling time is sufficiently long to be considered relevant for infection. An exact calculation of the falling time distribution is given in Appendix A, which shows that the relative standard deviation of the mean falling time is small for droplet radii larger than $R = 10 \text{ nm}$, thus the mean falling time τ_a in Eq. (1) is a good estimate of typical falling times for all droplets with $R > 10 \text{ nm}$.

Inertial effects due to the acceleration of a droplet that is initially at rest occur over the momentum diffusion or acceleration time, which is

$$\tau_{acc} = \frac{m D_R}{k_B T} = \frac{2\rho R^2}{9\eta} = \xi R^2 \quad , \quad (2)$$

where the numerical prefactor is given by $\xi = 8.37 \times 10^6 \text{ s m}^{-2}$. Even for large droplets with $R = 100 \text{ }\mu\text{m}$, the acceleration time is $\tau_{acc} = 0.1 \text{ s}$, showing that droplets rapidly reach their terminal velocity and acceleration effects can thus be neglected.

The lateral diffusion length during the time a droplet is floating in air is readily estimated. For this, the mean-squared diffusion length at the mean falling time is calculated from

$$x_D^2 = 2D_R \tau_a \text{ .}$$

Inserting the mean falling time from Eq. (1) results in

$$x_D = \sqrt{\frac{k_B T z_0}{4R^3 \rho g}} \text{ ,}$$

which yields $x_D = 0.3 \text{ mm}$ for a droplet of radius $R = 1 \text{ }\mu\text{m}$ and $x_D = 1 \text{ cm}$ for a droplet of radius $R = 100 \text{ nm}$. The lateral diffusion of a droplet during its lifetime is, therefore, very limited and will be dominated by the initial emission speed, wind and turbulent convection effects.

Note that the effect of evaporation has so far been neglected, which will decrease the droplet radius during its lifetime and therefore increase the time it takes for a droplet to reach the ground. For evaporation of a droplet at rest, which defines the so-called stagnant flow approximation, the time-dependent shrinking of the radius occurs in the diffusion-limited evaporation scenario, which is valid for radii larger than $R = 100 \text{ nm}$, and is given by (see Appendices B and C)

$$R(t) = R_0 (1 - \theta t (1 - RH) / R_0^2)^{1/2} \text{ .} \quad (3)$$

Here R_0 is the initial droplet radius and the numerical prefactor is given by

$$\theta = 2D_w c_g v_w \left(1 - \frac{\varepsilon_C \varepsilon_T}{1 + \varepsilon_C \varepsilon_T}\right) = 3.5 \times 10^{-10} \text{ m}^2/\text{s} \quad , \quad (4)$$

where θ has units of a diffusion constant. The values for the water diffusion constant in air D_w , the liquid water molecular volume v_w and the saturated water vapor concentration c_g at room temperature 25 °C are given in Table I. RH denotes the relative water humidity. The reduction of the water vapor concentration at the droplet surface due to evaporation cooling is described by the linear coefficient ε_C according to $c_g^{surf} \approx c_g(1 - \varepsilon_C \Delta T)$. Here c_g^{surf} denotes the water vapor concentration at the droplet surface, which has a temperature that is reduced compared to the ambient air by ΔT . The linear coefficient is given by $\varepsilon_C = 0.04$ (see Appendix C). The temperature reduction at the droplet surface is obtained by solving the coupled heat-flux and water diffusion-flux equations in a self-consistent manner and turns out to be linearly related to the relative humidity as $\Delta T = T_0 - T_s = \frac{\varepsilon_T(1-RH)}{1+\varepsilon_T\varepsilon_s} = 17(1 - RH)$, where the coefficient ε_T is given by $\varepsilon_T \equiv \frac{D_w c_g h_{ev}}{\lambda_{air}} = 52$ (see Appendix C). Interestingly, at zero relative humidity, $RH=0$, the droplet surface is cooled by 17 K, so for room temperature droplet freezing can be neglected. The factor in Eq. (4) that accounts for evaporation cooling effect is given by $\left(1 - \frac{\varepsilon_C \varepsilon_T}{1 + \varepsilon_C \varepsilon_T}\right) = 0.32$, cooling considerably slows down the evaporation process and cannot be neglected, see Appendices B and C for the derivation of Eq. (3).

Before the end of the drying process and if the radius becomes smaller than 100 nm, a crossover to the reaction-rate limited evaporation regime takes place, as will be discussed further below. From Eq. (3) it is seen that the decrease in the radius starts slowly and accelerates with time. Because of this, the time for evaporation to a radius, where osmotic effects due to dissolved solutes and the presence of virion particles within the droplet balance the water vapor chemical potential, can be approximated as the time needed to reduce the droplet radius to zero, given by

$$\tau_{ev} = \frac{R_0^2}{\theta(1-RH)} \quad . \quad (5)$$

This relation has been first established based on empirical grounds by Wells (3). Notably, the evaporation time in Eq. (5) increases quadratically with the initial droplet radius R_0 , while the falling time in Eq. (1) decreases inversely and quadratically with the radius. Thus, at a relative humidity of $RH = 0.5$, a common value for room air, a droplet with an initial radius of $R_0 = 10 \mu\text{m}$ has an evaporation time of $\tau_{ev} = 0.6 \text{ s}$, but needs (neglecting the reduction of the radius) $\tau_a = 170 \text{ s}$ to fall to the ground. Consequently, it will dry out and stay floating for an even longer time, depending on its final dry radius. A quick estimate of the critical radius below which droplets will completely dry out before falling to the ground is obtained by equating the floating and evaporation times in Eqs. (1) and (5), which gives

$$R^{crit} = (\varphi \theta z_0 (1 - RH))^{1/4} \quad . \quad (6)$$

Also this relation has been empirically established by Wells (3). For a relative humidity of $RH=0.5$ and an initial height of $z_0=2\text{m}$, the estimate $R^{crit} = 42 \mu\text{m}$ is obtained from Eq. (6). To accurately calculate the critical initial radius below which a droplet completely dries out

before falling to the ground, one needs to take into account the decrease in droplet radius due to evaporation while falling. Consequently, its diffusion constant and the change in gravitational force will change during its diffusive path towards the ground. The calculation is detailed in Appendix B and leads to the slightly modified result

$$R^{crit} = (2\phi\theta z_0(1 - RH))^{1/4} \quad . \quad (7)$$

For the critical radius at which a droplet has completely dried out when it hits the ground, one obtains from Eq. (7) for $RH=0.5$ and $z_0=2\text{m}$ the slightly higher estimate of $R^{crit} = 49 \mu\text{m}$. All droplets smaller than $R^{crit} = 49 \mu\text{m}$ will dry out before they hit the ground and shrink down to a radius that is predominantly determined by the solute content. Depending on the final size, they will be floating in air for an extended time given by Eq. (1). In airliners the relative humidity is substantially lower than 0.5; in fact, for completely dry air with $RH=0$ the critical radius increases to $R^{crit} = 59 \mu\text{m}$. Note that these arguments hold in still air, in air-conditioned rooms, convection due to air circulation will prevent some droplets from falling to the ground for a long time.

For droplets with radii smaller than $R=100 \text{ nm}$, the evaporation becomes dependent on the rate at which water evaporates from the droplet-air interface, this defines the so-called reaction-rate-limited evaporation regime. In Appendix D the radius in this regime shown to decrease as

$$R(t) = R_0 \left(1 - t \frac{k_c c_g v_w (1 - RH)}{R_0} \right) = R_0 (1 - \alpha^{reac} t (1 - RH) / R_0) \quad , \quad (8)$$

where R_0 is the initial droplet radius and the numerical prefactor is given by

$$\alpha^{reac} = k_c c_g v_w = 6.3 \times 10^{-3} \text{ m/s} \quad (9)$$

and has units of velocity. Here the evaporation cooling effect is neglected since heat transport stays diffusive and thus is faster than water transport. It is seen that the radius decrease is now linear in time, evaporation will stop at a radius when osmotic effects due to dissolved solutes and the presence of virions inside the droplet balance the evaporation chemical potential. The time needed to shrink the droplet to the final state can be approximated by

$$\tau_{ev}^{reac} = \frac{R_0}{\alpha^{reac}(1 - RH)} \quad . \quad (10)$$

For an initial radius of $R_0=100\text{nm}$, which is the upper limit where the stagnant reaction-limited evaporation regime is valid, the evaporation time is $\tau_{ev}^{reac} = 16 \mu\text{s} / (1 - RH)$. Thus, for relative humidity $RH=0.5$ the complete evaporation of a droplet with an initial radius of $R_0=100\text{nm}$ takes $32 \mu\text{s}$. This time is completely negligible compared to the floating time of a droplet with a radius of 100 nm , which is 20 days, and to the evaporation time of larger droplets. The final reaction-rate limited evaporation stage can thus be neglected for droplets significantly larger than 100 nm in radius.

For droplet radii larger than about $R = 60 \mu\text{m}$, non-linear hydrodynamic effects become important and produce a finite, so-called flow boundary layer, around the falling droplet.

Inside the flow boundary layer viscous effects are relevant and laminar flow is obtained, outside the flow boundary layer viscous effects can be neglected and potential flow is realized. At about the same range of radii, the stagnant approximation becomes invalid, because convection speeds up the evaporation process. This effect can be described by a concentration boundary layer. The problem is thus a double-boundary-layer problem and involves a concentration and a flow boundary layer (see Appendices E-H). Whether the concentration boundary layer or the flow boundary layer is smaller and thus more relevant, depends on the relative air humidity. It turns out that the evaporation in the presence of convection is diffusion limited. For humid air with a relative humidity $RH > 0.59$, the concentration boundary layer is evaporation-rate limiting and the time-dependent radius decrease is given by (see Appendix F)

$$R(t) = \left(R_0^{1/2} - \alpha^{dbl1} t (1 - RH)^{2/3} \right)^2, \quad (11)$$

where R_0 is the initial droplet radius and the numerical factor is given by

$$\alpha^{dbl1} = \frac{D_w c_g \left(1 - \frac{\varepsilon_C \varepsilon_T}{1 + \varepsilon_C \varepsilon_T} \right) v_w}{2 \Delta_0 R_*^{1/2}} = 1.8 \times 10^{-4} m^{1/2}/s. \quad (12)$$

Here $\Delta_0 = \left(\frac{9 \pi \eta D_w}{4 \rho g} \right)^{1/3} = 80 \mu m$ denotes the concentration boundary layer thickness in the absence of the flow boundary layer and $R_* = \left(\frac{9 \pi \eta^2}{4 g \rho_{air} \rho R^3} \right)^{1/3} = 59 \mu m$ denotes the critical radius for which the flow boundary layer thickness equals the radius. It is seen that the shrinking of the radius starts quickly and slows down over time. The estimate of the critical radius in Eq. (7) is located within the domain of validity of Eq. (3) and thus is valid. The evaporation cooling effect is approximately accounted for by a correction of the surface water vapor concentration by a factor $\left(1 - \frac{\varepsilon_C \varepsilon_T}{1 + \varepsilon_C \varepsilon_T} \right) = 0.32$, which accounts for the droplet surface temperature reduction.

For dry air with a relative humidity $RH < 0.59$, the flow boundary layer is evaporation-rate limiting and the time dependent radius decrease is given by

$$R(t) = \left(R_0^{1/2} - \alpha^{dbl2} t (1 - RH)^{1/2} \right)^2, \quad (13)$$

where the numerical factor is given by

$$\alpha^{dbl2} = \frac{D_w c_g \left(1 - \frac{\varepsilon_C \varepsilon_T}{1 + \varepsilon_C \varepsilon_T} \right) v_w}{2 \Delta_0^{3/2}} = 1.1 \times 10^{-4} m^{1/2}/s. \quad (14)$$

The evaporation cooling effect is again approximately accounted for by a correction of the surface water vapor concentration by a factor $\left(1 - \frac{\varepsilon_C \varepsilon_T}{1 + \varepsilon_C \varepsilon_T} \right) = 0.32$, which accounts for the droplet surface temperature reduction.

The results for the humid and dry boundary layer scenarios thus look quite similar, but the physical mechanisms behind the evaporation process are very different. At high Reynolds

numbers the friction experienced by a falling droplet is reduced due to a combination of boundary layer effects, boundary-layer separation effects and turbulence effects. In Appendix I it is shown that the Stokes expression for the friction acting on a falling spherical droplet is accurate for radii below about 160 μm .

So far, the finite solute concentration in the initial droplet, which produces a lower limit on the droplet radius that can be obtained by an evaporation process, has been neglected. For the example of saliva, which can be assumed to contain a mass percentage of about 99.5 % water, a droplet can maximally shrink by a factor $200^{1/3} = 6$. Thus, neglecting the solute-induced water vapor pressure reduction for the moment, droplets with an initial radius of about $R = 30 \mu\text{m}$ will for $RH=1/2$ shrink down to a final radius $R_\infty = 5 \mu\text{m}$ during the evaporation time $\tau_{ev} = 5.4 \text{ s}$, as approximately given by Eq. (5), and then sediment for about 11 minutes, as predicted by Eq. (1) for an initial height of $z_0=2 \text{ m}$. Some of the water will stay inside the final droplet because of hydration effects. Assuming that the final state contains 50% strongly bound hydration water, the droplet can maximally shrink by a factor of $100^{1/3} = 5$. Thus, in this scenario, droplets with an initial radius of about $R= 25 \mu\text{m}$ shrink for $RH=1/2$ down to a radius $R_\infty = 5 \mu\text{m}$ in $\tau_{ev} = 3.8 \text{ s}$, as given by Eq. (5), and then sediment for about 11 minutes. It is important to note that the concentration of non-volatile solutes (including virions) has in the latter example increased by a factor of 100 due to evaporation.

Solutes in the droplet decrease the water vapor pressure, as predicted by Raoult's law, and therefore limit the equilibrium droplet radius that is obtained in the long-time limit according to

$$R_\infty = R_0 \left(\frac{\Phi_0}{1-RH} \right)^{1/3} . \quad (15)$$

Here, R_0 is the initial radius and Φ_0 is the initial volume fraction of solutes. Only for $RH=0$ does a droplet dry out to the minimal possible radius of $R_\infty = R_0(\Phi_0)^{1/3}$, for finite relative humidity the equilibrium droplet radius is characterized by an equilibrium solute volume fraction of $\Phi_\infty = 1 - RH$. As an example, for $RH=1/2$, the water and solute volume fractions in the equilibrium state equal each other. Equation (15) is modified for solutes that perturb the water activity, but for most solutes non-ideal water solution effects can be neglected. To illustrate this: the saturation concentration of NaCl in water is approximately 6M, which corresponds, for simplicity assuming equal volume of Na^+ cations, Cl^- anions and water molecules, roughly to a volume fraction of $\Phi_\infty = 12\text{M}/(55+12)\text{M} = 0.18$, thus suggesting a water vapor pressure of $RH = 1 - \Phi_\infty = 0.82$, which is rather close to the experimental water vapor pressure of a saturated NaCl solution of 0.75.

Taking into account the water vapor pressure reduction during the evaporation process, the analytical result for the radius-dependent evaporation time, which is the time it takes for the droplet radius to decrease from its initial value R_0 down to R , is given by

$$t(R) = \frac{R_\infty^2}{\theta(1-RH)} \left[\mathcal{L} \left(\frac{R_0}{R_\infty} \right) - \mathcal{L} \left(\frac{R}{R_\infty} \right) \right] , \quad (16)$$

as derived in Appendix K. A very accurate yet simple approximation for the scaling function $\mathcal{L}(x)$ is

$$\mathcal{L}\left(\frac{R}{R_\infty}\right) \cong \left(\frac{R}{R_\infty}\right)^2 + \frac{2}{3} \ln\left(1 - \frac{R_\infty}{R}\right) \quad , \quad (17)$$

with which Eq. (16) can be written as

$$t(R)/\tau_{ev} = 1 - \frac{R^2}{R_0^2} - \frac{2R_\infty^2}{3R_0^2} \ln\left(\frac{R_0(R-R_\infty)}{R(R_0-R_\infty)}\right) \quad , \quad (18)$$

where τ_{ev} denotes the evaporation time to shrink the solute-free droplet down to a vanishing radius from Eq. (5). This expression clearly illustrates the logarithmic slowing down of the evaporation process due to the increasing solute concentration as the droplet radius R approaches the equilibrium droplet radius R_∞ . Neglecting the finite final radius, i.e. setting $R_\infty = 0$, valid for pure water droplets, the last term in Eq. (18) vanishes and one obtains the limiting result

$$t(R)/\tau_{ev} = 1 - \frac{R^2}{R_0^2} \quad . \quad (19)$$

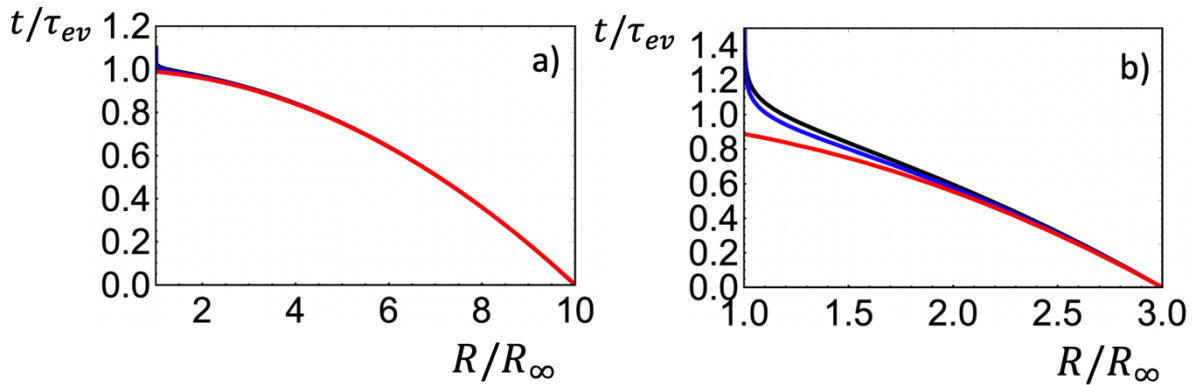


Fig. 1: Scaling plot of the evaporation time $t(R)$ as a function of the radius R in the presence of solutes according to Eq. (16) (black lines). In a) the ratio of the initial droplet radius to the final equilibrium radius is $\frac{R_0}{R_\infty} = 10$ and in b) this ratio is $\frac{R_0}{R_\infty} = 3$. The red lines show the evaporation time when the water vapor pressure reduction is neglected, Eq. (19), the blue lines show the approximation Eq. (18). The solute-induced water-vapor pressure reduction becomes significant only for radii close to the final equilibrium radius R_∞ and leads to a diverging evaporation time.

Figure 1 shows the rescaled evaporation time as a function of the reduced droplet radius according to Eq. (16) as black lines. The presence of solutes only becomes relevant for droplet radii that are close to the final equilibrium radius R_∞ and gives rise to a divergent evaporation time. Except this final stage of evaporation, the formula Eq. (19) (red lines) describes the evaporation very accurately. The threshold radius below which the presence of solutes becomes important, can be defined by the radius where the function $t(R)$ changes curvature. The second derivative of $t(R)$ in Eq. (18) is given by

$$\frac{R_0^2 d^2 t(R)/\tau_{ev}}{dR^2} = -2 + \frac{2}{3} \left((1 - R/R_\infty)^{-2} - (R/R_\infty)^{-2} \right) \quad , \quad (20)$$

and vanishes at a radius of $R/R_\infty = 1.54$. Thus, according to this curvature criterion, droplets enter the solute-dominated evaporation regime for radii smaller than $R = 1.54 R_\infty$, independent of the initial droplet radius R_0 .

So far it has been assumed that diffusion within the droplet happens quickly enough, so that the water concentration at the droplet surface does not differ significantly from the mean water concentration in the droplet. In Appendix J it is shown that this is a limiting factor for the maximal droplet size that can evaporate before reaching the ground. In fact, the mixing time inside the droplet is only shorter than the falling time for initial radii smaller than $R=100 \mu\text{m}$. For larger droplets, the internal diffusion will slow down or even stop evaporation when the solubility limit at the droplet surface has been reached, in this case the droplet might sink to the ground without evaporation taking place at a sufficient rate. The increase of the internal droplet viscosity as the solute concentration rises due to evaporation and the possible presence of a solid solute phase will further slowdown evaporation, which are additional effects that have not been considered here.

Surface tension effects, which increase the water vapor pressure, are negligible for droplets with radii larger than $R = 1\text{nm}$, as explained in Appendix L.

In summary, the evaporation of aqueous droplets with radii above $60 \mu\text{m}$ proceeds in three subsequent stages: i) for radius $R > 60 \mu\text{m}$, the evaporation proceeds via boundary layer evaporation in the simultaneous presence of a fluid and a concentration boundary layer, and is described by Eq. (11) or (13), depending on the relative humidity; ii) for $100 \text{ nm} < R < 60 \mu\text{m}$, which is the most important radius regime for air-borne infection pathways, evaporation is described by the stagnant approximation in the diffusion limit, Eq. (3); iii) for radii $R < 100 \text{ nm}$ the evaporation is reaction-rate limited and described by Eq. (8). The critical radius at which a droplet has completely dried out when it hits the ground follows for intermediate droplet radii $100 \text{ nm} < R < 60 \mu\text{m}$ from Eq. (7) and is given for relative humidity $RH=0.5$ and initial height $z_0=2\text{m}$ by $R^{\text{crit}} = 49 \mu\text{m}$. Droplets smaller than $R^{\text{crit}}= 49 \mu\text{m}$ will dry out before they hit the ground and shrink down to a radius that is determined by the solute content, given by Eq. (15), and stay floating in air for an extended time given by Eq. (1). The relative humidity plays an important role, for completely dry air with $RH=0$ the critical radius increases to $R^{\text{crit}} = 59 \mu\text{m}$. These calculations demonstrate in terms of analytical formulas, that droplets in the entire range of radii below about $R^{\text{crit}}= 49 \mu\text{m}$ for $RH=1/2$, will shrink significantly before they fall to the ground and thus stay floating in air longer than their initial radius would suggest. Measurements of droplet size distributions suggest that the majority of droplets produced during coughing and speaking have radii in this range, therefore the droplet evaporation effects discuss here are relevant for accurate estimates of the air-borne infection risk. The analytical formulas presented in this work will facilitate further calculations of droplet dwelling times that include convection and turbulent flow effects.

$k_B T$	thermal energy	$4.1 \times 10^{-21} \text{ J at } 25^\circ\text{C}$
η	viscosity of air	$1.86 \times 10^{-5} \text{ kg/ms at } 25^\circ\text{C}$
η	viscosity of air	$1.73 \times 10^{-5} \text{ kg/ms at } 0^\circ\text{C}$
ρ	liquid water density	10^3 kg/m^3

g	gravitational constant	9.81 m/s^2
D_w	water diffusion constant in air	$2.82 \times 10^{-5} \text{ m}^2/\text{s}$ at 25°C
D_w	water diffusion constant in air	$2.2 \times 10^{-5} \text{ m}^2/\text{s}$ at 0°C
D_w^l	water diffusion constant in liquid water	$2.3 \times 10^{-9} \text{ m}^2/\text{s}$ at 25°C
m_w	water molecular mass	$2.99 \times 10^{-26} \text{ kg}$
v_w	liquid water molecular volume	$3.07 \times 10^{-29} \text{ m}^3$ at 25°C
v_w	liquid water molecular volume	$2.99 \times 10^{-29} \text{ m}^3$ at 4°C
c_g	saturated vapor water concentration	$6.6 \times 10^{23} \text{ m}^{-3}$ at 25°C
P_{vap}	water vapor pressure	2340 Pa at 20°C
P_{vap}	water vapor pressure	610 Pa at 0°C
ρ_{air}	density of air is given by	1.18 kg m^{-3} at 25°C
ν	Kinematic air viscosity	$1.5 \times 10^{-5} \text{ m}^2/\text{s}$ at 25°C
k_c	condensation reaction rate coefficient	300 m/s
a_{air}	air temperature diffusivity	$2 \times 10^{-5} \text{ m}^2/\text{s}$
a_w	Liquid water temperature diffusivity	$1.4 \times 10^{-7} \text{ m}^2/\text{s}$
h_{ev}	molecular evaporation enthalpy of water	$7.3 \times 10^{-20} \text{ J}$ at 25°C
h_{ev}	molecular evaporation enthalpy of water	$7.1 \times 10^{-20} \text{ J}$ at 0°C
h_m	molecular melting enthalpy of water	$1.0 \times 10^{-20} \text{ J}$
C_p^l	molecular heat capacity of liquid water	$1.3 \times 10^{-22} \text{ J}$ at 25°C
λ_{air}	heat conductivity of air	0.026 W/mK at 25°C
λ_{air}	heat conductivity of air	0.024 W/mK at 0°C

Acknowledgements: I thank William Eaton for helpful comments and for bringing this problem to my attention. Discussions with A. Bax, I. Gersonde and P. Loche are gratefully acknowledged. This research has been funded by Deutsche Forschungsgemeinschaft (DFG) through grant CRC 1114 "Scaling Cascades in Complex Systems", grant Number 235221301, Project C02 and by the ERC Advanced Grant No. 835117.

References

1. **Anfinrud, P. A., Stadnytskyi, V., Bax, C. E. and Bax, A.** Visualizing speech-generated oral fluid droplets with laser light scattering. *New Engl. J. Med.* 2020, p. DOI: 10.1056/NEJMc2007800.
2. **Frössling, N.** Über die Verdunstung fallender Tropfen. *Gerlands Beitr. Geophysik.* 1938, Vol. 52, p. 170.
3. **Wells, W. F.** On Air-Borne Infection. Study II: Droplets and Droplet Nuclei. *Am. J. Hyg.* 1934, Vol. 20, p. 611.
4. **Duguid, J.P.** The size and the duration of air-carriage of respiratory droplets and droplet-nuclei. *J. Hyg.* 1946, Vol. 4, p. 471.
5. **Kinzer G. D. and Gunn, R.** The evaporation, temperature and thermal relaxation-time of freely falling waterdrops. *J. Meteorology.* 1951, Vol. 8, p. 71.
6. **Best, A. C.** The evaporation of raindrops. *Quart. J. Roy. Meteorol. Soc.* 1952, Vol. 78, p. 200.
7. **Ranz, W. E. and Marshall, W. R.** Evaporation from drops. *Chem. Eng. Progr.* 1952, Vol. 48, p. 141.

8. **Kukkonen, J., Vesala, T. and Kulmala, M.** The interdependence of evaporation and settling for airborne freely falling droplets. *J. Aerosol Sci.* 1989, Vol. 20, p. 749.
9. **Xie, X., Li, Y., Chwang, A. T. Y., Ho, P. ,L. and Seto, W. H.** How far droplets can move in indoor environments - revisiting the Wells evaporation-falling curve. *Indoor Air.* 2007, Vol. 17, p. 211.
10. **Liu, L., Wei, J., Li, Y. and Ooi, A.** Evaporation and dispersion of respiratory droplets from coughing. *Indoor Air.* 2017, Vol. 27, p. 179.
11. **Redrow, J., Shaolin Mao, S., Celik, I., Posada, J. A., Feng, Z.-G.** Modeling the evaporation and dispersion of airborne sputum droplets expelled from a human cough. *Building and Environment.* 2011, Vol. 46, p. 2042.
12. **Fuchs, N. A.** Evaporation and droplet growth in gaseous media. *Pergamon Press, London.* 1959.
13. **Papineni, R. S. and Rosenthal, F. S.** The size distribution of droplets in the exhaled breath of healthy human subjects. *J. Aerosol Med.* 1997, Vol. 10, p. 105.
14. **Yang, S., Lee, G. W. M., Chen, C.-M., Wu, C.-C. and Yu, K.-P.** The size and concentration of droplets generated by coughing in human subjects. *J. Aerosol Med.* 2007, Vol. 20, p. 484.
15. **Xie, X., Li, Y., Sun, H. and Liu, L.** Exhaled droplets due to talking and coughing. *J. R. Soc. Interface.* 2009, Vol. 6, p. S703.
16. **Zhang, H., Li, D., Xie, L. and Xiao, Y.** Documentary research of human respiratory droplet characteristics. *Proc. Eng.* 2015, Vol. 121, p. 1365.
17. **Chao, C. Y. H., Wan, M. P., Morawska, L., Johnson, G. R., Ristovski, Z. D., Hargreaves, M., Mengersen, K., Corbett, S., Li, Y., Xie, X., Katoshevski, D.** Characterization of expiration air jets and droplet size distributions immediately at the mouth opening. *Aerosol Science.* 2009, Vol. 40, p. 122.
18. **Gralton, J., Tovey, E., McLaws, M.-L., Rawlinson, W. D.** The role of particle size in aerosolised pathogen transmission: A review. *Journal of Infection.* 2011, Vol. 62, p. 1.
19. **Johnson, G.R., Morawska, L., Ristovskia, Z.D., Hargreaves, M., Mengersen, K., Chao, C.Y. H., Wan, M. P, Li, Y., Xie, X., Katoshevski, D., Corbett, S.** Modality of human expired aerosol size distributions. *Journal of Aerosol Science.* 2011, Vol. 42, p. 839.
20. **Asadi, S., Wexler, A. S., Cappa, C. D., Barreda, N. M., Bouvier, N. M. and Ristenpart, W. D.** Aerosol emission and superemission during human speech increase with voice loudness. *Scientific Reports.* 2019, Vol. 9, p. 2348.
21. **Scharfman, B. E., Techet, A. H., Bush, J. W. M. and Bourouiba, L.** Visualization of sneeze ejecta: steps of fluid fragmentation leading to respiratory droplets. *Exp. Fluids.* 2016, Vol. 57, p. 24.
22. **van Doremalen, N., Bushmaker, T., Morris, D. H., Holbrook, M. G., Gamble, A., Williamson, B. N., Tamin, A., Harcourt, J. L., Thornburg, N. J., Gerber, S. I., Lloyd-Smith, J. O., de Wit, E. and Munster, V. J.** Aerosol and Surface Stability of SARS-CoV-2 as Compared with SARS-CoV-1. *The new england journal of medicine.* 2020, Vol. 382, p. 16.
23. **Shamana, J., and Kohn, M.** Absolute humidity modulates influenza survival, transmission, and seasonality. *PNAS.* 2009, Vol. 106, p. 3243.
24. **Tellier, R.** Aerosol transmission of influenza A virus: a review of new studies. *J. R. Soc. Interface.* 2009, Vol. 6, p. S783.
25. **Ai, Z. T. and Melikov, A. K.** Airborne spread of expiratory droplet nuclei between the occupants of indoor environments: A review. *Indoor Air.* 2018, Vol. 28, p. 500.
26. **Batchelor, G. K.** An Introduction to Fluid Dynamics. *Cambridge University Press, Cambridge.* 1967.

Appendix A: Diffusive droplet falling without evaporation

The density distribution of droplets that diffuse in a viscous medium (such as air) under the influence of gravitational force is given by the diffusion equation

$$\frac{d}{dt} P(z, t) = D_R \frac{d^2}{dz^2} P(z, t) + V \frac{d}{dz} P(z, t), \quad (\text{A1a})$$

where the stationary velocity is defined as

$$V = \frac{D_R m g}{k_B T} \quad (\text{A1b})$$

and D_R is the droplet diffusion coefficient, m the droplet mass, g the gravitational acceleration, $k_B T$ the thermal energy and $P(z, t)$ is the density of droplets at height z and time t . The fact that droplets do not return to air once they reach the ground at height $z=0$ is accounted for by a vanishing density distribution at the ground, $P(z=0, t)=0$, which is the absorbing boundary condition. The Laplace-transformed density distribution at time t , given that at time $t=0$ droplets are placed at height z_0 , the so-called Green's function, is given by

$$\tilde{P}(\omega, z|z_0) = \frac{(e^{\gamma_1 z_0} - e^{-\gamma_2 z_0}) e^{-\gamma_1 z}}{\sqrt{V^2 + 4D_R \omega}} \quad \text{for } z > z_0 \quad (\text{A2a})$$

$$\tilde{P}(\omega, z|z_0) = \frac{e^{-\gamma_2 z_0} (e^{\gamma_2 z} - e^{-\gamma_1 z})}{\sqrt{V^2 + 4D_R \omega}} \quad \text{for } z < z_0, \quad (\text{A2b})$$

where the decay lengths are defined as

$$\gamma_1 = \sqrt{\frac{V^2}{4D_R^2} + \frac{\omega}{D_R}} + \frac{V}{2D_R}$$

$$\gamma_2 = \sqrt{\frac{V^2}{4D_R^2} + \frac{\omega}{D_R}} - \frac{V}{2D_R}.$$

The survival fraction of droplets, i.e. the fraction of droplets that have not yet reached the ground, is obtained by the integral over the entire density distribution and given by

$$\tilde{S}(\omega, z_0) = \int_0^\infty dz \tilde{P}(\omega, z|z_0) = \left(\frac{4D_R}{V^2}\right) \frac{1 - e^{-\tilde{z}_0[\sqrt{1+\tilde{\omega}}-1]/2}}{\tilde{\omega}}, \quad (\text{A3})$$

where rescaled variables $\tilde{z}_0 = \frac{z_0 V}{D_R}$ and $\tilde{\omega} = \frac{4\omega D_R}{V^2}$ are introduced. The inverse Laplace transform reads in closed form

$$S(t, z_0) = \frac{2D_R}{V^2} \left[1 - \operatorname{erf} \left(\frac{\tilde{t}^{\frac{1}{2}} - \frac{\tilde{z}_0 \tilde{t}^{-\frac{1}{2}}}{4}}{\tilde{t}^{\frac{1}{2}} - \frac{\tilde{z}_0 \tilde{t}^{-\frac{1}{2}}}{4}} \right) - e^{-\tilde{z}_0} \operatorname{erfc} \left(\frac{\tilde{t}^{\frac{1}{2}} - \frac{\tilde{z}_0 \tilde{t}^{-\frac{1}{2}}}{4}}{\tilde{t}^{\frac{1}{2}} - \frac{\tilde{z}_0 \tilde{t}^{-\frac{1}{2}}}{4}} \right) \right], \quad (\text{A4a})$$

where $\tilde{\omega} \tilde{t} = \omega t$, and has for large times the asymptotic decay

$$S(t, z_0) \sim z_0 t^{-3/2} e^{-V^2 t/4D_R} . \quad (A4b)$$

This shows that all higher moments exist. The absorption time distribution is given by

$$K(t, z_0) = -\frac{\partial S(t, z_0)}{\partial t} \quad (A5)$$

and is normalized. The first moment of the absorption distribution, the mean absorption time, is given by

$$\tau_a = \int_0^\infty dt t K(t, z_0) = \int_0^\infty dt S(t, z_0) = \tilde{S}(\omega, z_0)|_{\omega \rightarrow 0} . \quad (A6)$$

Likewise, the second moment is given by

$$\tau_a^{(2)} = \int_0^\infty dt t^2 K(t, z_0) = 2 \int_0^\infty dt t S(t, z_0) = -2 \frac{\partial \tilde{S}(\omega, z_0)}{\partial \omega} |_{\omega \rightarrow 0} . \quad (A7)$$

The explicit result for the mean adsorption time therefore reads

$$\tau_a = \frac{z_0}{V} = \frac{k_B T z_0}{D_R m g} \quad (A8)$$

and is the expected time for a droplet falling with constant velocity V to reach the ground. The thermal equilibrium mean-height of a droplet above the ground (in the absence of absorption) is from the equipartition theorem given by

$$z_{eq} = \frac{k_B T}{m g} . \quad (A9)$$

Using $m = 4\pi R^3 \rho/3$ and numerical constants from Table I, for droplet radii $R = 1$ nm, 10 nm, 100 nm equilibrium heights of $z_{eq} = 100$ m, 100 mm, 100 μ m are obtained, so it is seen that thermal effects can be safely neglected for all but the smallest droplets. The relative standard deviation of the absorption time follows from Eq. (A7) as

$$\frac{\Delta \tau_a}{\tau_a} = \frac{\sqrt{\tau_a^{(2)} - \tau_a^2}}{\tau_a} = \sqrt{\frac{2z_{eq}}{z_0}} . \quad (A10)$$

Together with the result Eq. (A9), the relative standard deviation is seen to be small for droplets larger than $R=10$ nm and for an initial height z_0 in the meter range.

Appendix B: Stagnant droplet evaporation in the diffusion-limited regime without evaporation cooling effects

In this appendix, convection effects in the air around the droplet due to the finite speed of a falling droplet will be neglected, which increase the speed of evaporation and will be treated in Appendices E-H. The water vapor concentration around a spherical droplet at rest is described by the diffusion equation in radial coordinates

$$\frac{d}{dt}c(r, t) = \frac{D_w}{r^2} \frac{d}{dr} r^2 \frac{d}{dr} c(r, t) , \quad (\text{B1})$$

where D_w denotes the molecular water diffusion constant in air. The stationary density distribution is given by

$$c(r) = c_0 \left(1 + \frac{b}{r} \right) , \quad (\text{B2})$$

where c_0 is the ambient water vapor concentration. Here the adiabatic approximation is used and the time it takes for the stationary distribution to build up, which can be shown to be small, is neglected. Particle conservation together with the reactive boundary condition at the droplet surface $r=R$ gives for the flux density j

$$j = -D_w \frac{d}{dr} c(R) = k_e c_l - k_c c(R) , \quad (\text{B3})$$

where k_e and k_c are the evaporation and condensation reaction rate coefficients, which have units of velocity, and c_l is the liquid water concentration inside the droplet (or, to be more precise, at the droplet surface). Inserting the solution Eq. (B2) into Eq. (B3), the resulting equation can be solved for the coefficient b and the total water evaporation flux, J , is obtained as

$$J = 4\pi R^2 j = 4\pi D_w c_0 b = 4\pi R^2 D_w \frac{k_e c_l - k_c c_0}{D_w + k_c R} . \quad (\text{B4})$$

For saturated water vapor with concentration c_g , the evaporation flux must vanish, i.e. $k_e c_l = k_c c_g$, and the evaporation rate coefficient k_e can be eliminated from Eq. (B4) to give

$$J = 4\pi R^2 D_w \frac{k_c c_g (1 - RH)}{D_w + k_c R} , \quad (\text{B5})$$

where the relative fractional air humidity is defined as $RH = c_0/c_g$. As expected, the evaporation flux vanishes for $RH = 1$ of saturated air. The condensation reaction rate coefficient k_c is large, since every water molecule that hits the air-water interface basically sticks. From molecular kinetic considerations, it follows that k_c is given by the thermal molecular water velocity

$$k_c = \sqrt{\frac{k_B T}{m_w}} \approx 300 \text{ m/s} , \quad (\text{B6})$$

where the water molecule mass m_w from Table I was used. The diffusion-limited rate scenario is defined by $k_c R > D_w$, which is realized for droplet radii $R > \frac{D_w}{k_c} = 100 \text{ nm}$, where the water molecular diffusion constant in air, D_w at 25°C from Table I, was used. In this limit, one can neglect the term proportional to D_w in the denominator of Eq. (B5) and obtains the classical diffusion-limited result for the evaporation flux, which is linearly proportional to the droplet radius,

$$J = 4\pi R D_w c_g (1 - RH) . \quad (\text{B7})$$

Mass conservation of the droplet means that the evaporation flux is balanced by a decreasing radius, which can be written in terms of the droplet volume as

$$\frac{d}{dt} \left(\frac{4\pi}{3} R^3(t) \right) = -v_w J = -4\pi R D_w c_g v_w (1 - RH) \quad , \quad (B8)$$

where v_w is the volume of a water molecule in the liquid phase. The differential equation (B8) is easily solved with the result

$$R(t) = R_0 \left(1 - t \frac{2D_w c_g v_w (1-RH)}{R_0^2} \right)^{1/2} = R_0 (1 - \theta t (1 - RH) / R_0^2)^{1/2} \quad , \quad (B9)$$

where R_0 is the initial droplet radius and the numerical prefactor is given by

$$\theta = 2D_w c_g v_w = 1.1 \times 10^{-9} m^2 / s \quad (B10)$$

and has units of a diffusion constant. Note that the calculation neglects evaporation cooling effects, which substantially change the numerical prefactor, as shown in Appendix C. The water molecular volume in the liquid phase, v_w , and the water concentration of saturated water vapor, c_g , have been taken from Table I. It is seen that the shrinking of the radius starts slowly and accelerates over time. The evaporation time down to a radius where osmotic effects due to dissolved solutes and the presence of virions inside the droplet balance the evaporation chemical potential, can thus be approximated as the time needed to shrink the droplet radius down to zero, given by

$$\tau_{ev} = \frac{R_0^2}{\theta(1-RH)} \quad . \quad (B11)$$

Notably, the evaporation time in Eq. (B11) increases quadratically with the initial droplet radius R_0 , while the absorption time in Eq. (1) decreases inversely and quadratically with R_0 . Thus, at a relative humidity of $RH=0.5$, a common value for room air, a droplet with an initial radius of $R_0=1 \mu m$ has an evaporation time of $\tau_{ev} = 1.8$ ms, but needs (neglecting shrinkage of the radius) $\tau_a=5$ h to fall to the ground, so it will dry out and basically stay floating for an even longer time, depending on its final dry radius.

To calculate the critical initial radius below which a droplet completely dries out before falling to the ground, Eq. (1) is rewritten in terms of the instantaneous, radius-dependent droplet velocity $v(t)$ and combined with Eq. (B9) as

$$v(t) = \frac{D_R g m(t)}{k_B T} = \frac{R^2(t)}{\varphi} = \frac{R_0^2}{\varphi} (1 - \theta t (1 - RH) R_0^{-2}) \quad . \quad (B12)$$

The distance by which the droplet falls during its evaporation time τ_{ev} follows by integration as

$$\Delta z = \int_0^{\tau_{ev}} v(t) dt = \frac{R_0^4}{2\theta\varphi(1-RH)} \quad . \quad (B13)$$

Now equating the distance Δz with the initial height z_0 , the critical droplet radius follows as

$$R^{crit} = (2\phi\theta z_0(1 - RH))^{1/4} . \quad (B14)$$

Droplets with radii smaller than R^{crit} will completely dry out before reaching the ground. Note that this formula neglects the finite solute concentration in the initial droplet, which will be considered in Appendix K and produces a lower limit to the droplet radius that can be obtained by evaporation.

Appendix C: Stagnant droplet evaporation in the diffusion-limited regime with evaporation cooling effects

There are several effects that temperature has on evaporation kinetics. The temperature diffusion constant is defined as $a = \lambda/(cC_p)$, where λ is the heat conductivity coefficient, c is the number density and C_p is the molecular heat capacity at constant pressure. For air one finds a value $a_{air} = 2 \times 10^{-5} \text{ m}^2/\text{s}$, which is very similar to the water diffusion constant in air (see Table I). Thus, temperature gradient effects cannot necessarily be neglected. The fact that evaporation cooling is relevant can be appreciated quickly: The molecular evaporation enthalpy of water at 25°C is $h_{ev} = 7.3 \times 10^{-20} \text{ J}$, the molecular heat capacity of liquid water at 25°C is $C_p^l = 1.3 \times 10^{-22} \text{ J}$, so one evaporating water molecules cools down 20 liquid water molecules from 25°C to 0°C. The molecular melting enthalpy of water is $h_m = 1.0 \times 10^{-20} \text{ J}$, so one evaporating water molecules freezes 7 liquid water molecules. One sees that cooling due to evaporation needs to be accounted for.

The temperature profile around a spherical heat sink is described by the heat diffusion equation in radial coordinates

$$cC_p \frac{d}{dt} T(r, t) = \frac{\lambda_{air}}{r^2} \frac{d}{dr} r^2 \frac{d}{dr} T(r, t) , \quad (C1)$$

where λ_{air} denotes the heat conductivity of air. The stationary temperature distribution is given by

$$T(r) = T_0 \left(1 - \frac{b_T}{r} \right) , \quad (C2)$$

where T_0 is the ambient temperature, from which the droplet surface temperature follows as

$$T_s = T_0 \left(1 - \frac{b_T}{R} \right) . \quad (C3)$$

The adiabatic approximation is used, meaning that the time it takes for the stationary temperature distribution to build up, is neglected; this is justified since the heat capacity of the droplet is small compared to the evaporation enthalpy, as shown above. After a few water molecules have evaporated, the droplet will have a uniform temperature equal to the air close to the surface. The heat flux into the droplet is given by

$$J_h = 4\pi R^2 \lambda_{air} \frac{d}{dR} T(R) = 4\pi \lambda_{air} T_0 b_T . \quad (C4)$$

In a stationary state, the thermal heat flux exactly balances the evaporation cooling rate, which is the water evaporation rate J from Eq. (B5) times the evaporation enthalpy. The energy balance equation reads explicitly

$$J_h = h_{ev}J = 4\pi R^2 h_{ev} D_w \frac{k_e c_l - k_c c_0}{D_w + k_c R} = 4\pi R^2 h_{ev} D_w \frac{k_c c_g (1 - RH)}{D_w + k_c R} . \quad (C5)$$

In the diffusion-limited scenario this leads to

$$J_h = h_{ev}J = 4\pi R h_{ev} D_w c_g (1 - RH) . \quad (C6)$$

Combining Eqs. (C3), (C4) and (C6), one obtains for the temperature depression at the droplet surface

$$\Delta T = T_0 - T_s = \frac{D_w c_g h_{ev}}{\lambda_{air}} (1 - RH) = \varepsilon_T (1 - RH) , \quad (C7)$$

where the numerical prefactor is for air given by $\varepsilon_T \equiv \frac{D_w c_g h_{ev}}{\lambda_{air}} = 52$. This is a surprising result, as it would suggest that the evaporation of a droplet leads to droplet freezing at room temperature at all but very high relative humidity.

The estimate in Eq. (C7) neglects that there counteracting effects that decrease the evaporation rate with decreasing temperature. Inspection of Table I and noting that the water vapor concentration is linearly proportional to the water vapor pressure, shows that the dominant temperature effect in Eq. (C6) comes from the saturated water vapor concentration c_g , which is related to the liquid water density according to

$$c_g = c_l e^{\mu_{ex}/k_B T} . \quad (C8)$$

The saturated water vapor concentration c_g thus depends on the liquid water concentration c_l (which depends only slightly on temperature) and exponentially on the water excess chemical potential, which at room temperature is given by $\mu_{ex} = -\frac{27\text{kJ}}{\text{mol}}$ and decreases significantly with decreasing temperature, showing that c_g quickly goes down as the temperature decreases. In the temperature range between 0°C and 25°C the surface water vapor concentration can be linearly fitted according to

$$c_g^s = c_g (1 - \varepsilon_c \Delta T) , \quad (C9)$$

with a numerical prefactor $\varepsilon_c = 0.037 = (2340 - 610)/(20 \times 2340)$, which is obtained by linear interpolation of the water vapor pressure at 0°C, $P_v = 0.61$ kPa, and at 20°C, $P_v = 2.34$ kPa, see Table I. Replacing c_g by c_g^s in Eq. (C6), the final result for the temperature depression at the droplet surface follows from solving the energy balance equation Eq. (C6) in a self-consistent manner, which gives

$$\Delta T = T_0 - T_s = \frac{\varepsilon_T (1 - RH)}{1 + \varepsilon_T \varepsilon_c} = 17(1 - RH) . \quad (C10)$$

One sees that the temperature reduction at the droplet surface is, including the temperature dependence of the water vapor concentration at the droplet surface, less

pronounced and for RH=0.5 is about 9 K. Thus, freezing is preempted and the linearization of the water vapor concentration in Eq. (C9) is valid.

In the presence of evaporation-induced droplet cooling, the diffusional water flux is obtained from Eq. (C6) as

$$J = 4\pi R D_w (c_g^s - c_0) = 4\pi R D_w (c_g(1 - \varepsilon_C \Delta T) - c_0), \quad (C11)$$

which using Eq. (C10) can be rewritten as

$$J = 4\pi R D_w c_g \left(1 - \frac{\varepsilon_C \varepsilon_T}{1 + \varepsilon_C \varepsilon_T}\right) (1 - RH). \quad (C12)$$

Repeating the steps that led to Eq. (B9) in Appendix B, one obtains the modified evolution equation for the radius

$$R(t) = (1 - \theta t(1 - RH)/R_0^2)^{1/2}, \quad (C13)$$

where the modified numerical prefactor is given by

$$\theta = 2D_w c_g v_w \left(1 - \frac{\varepsilon_C \varepsilon_T}{1 + \varepsilon_C \varepsilon_T}\right) = 3.5 \times 10^{-10} m^2/s. \quad (C14)$$

The factor that self-consistently accounts for the evaporation cooling effect is thus given by $\left(1 - \frac{\varepsilon_C \varepsilon_T}{1 + \varepsilon_C \varepsilon_T}\right) = 0.32$, cooling considerably slows down the evaporation process but does not lead to droplet freezing.

Appendix D: Stagnant droplet evaporation in the reaction-rate-limited regime

To obtain the evaporation flux in the reaction-rate limited regime, one starts from Eq. (B5) and assumes $k_c R < D_w$, which is realized for droplet radii $R < \frac{D_w}{k_c} = 100 \text{ nm}$, see the discussion after Eq. (B6). In this limit one can neglect the term proportional to $k_c R$ in the denominator of Eq. (B5) and obtains the reaction-rate-limited result for the flux, which is proportional to R^2 and thus the surface area of the droplet,

$$J = 4\pi R^2 k_c c_g (1 - RH) \quad . \quad (D1)$$

Mass conservation of the droplet reads

$$\frac{d}{dt} \left(\frac{4\pi}{3} R^3(t) \right) = -v_w J = -4\pi R^2 k_c c_g v_w (1 - RH) \quad . \quad (D2)$$

The differential equation (D2) is easily solved with the result

$$R(t) = R_0 \left(1 - t \frac{k_c c_g v_w (1 - RH)}{R_0}\right) = R_0 (1 - \alpha^{reac} t(1 - RH)/R_0) \quad , \quad (D3)$$

where R_0 is the initial droplet radius and the numerical prefactor is given by

$$\alpha^{react} = k_c c_g v_w = 6.3 \times 10^{-3} m/s \quad (D4)$$

and has units of a velocity. It is seen that shrinking of the radius now is linear in time, evaporation will stop at a radius when osmotic effects due to dissolved solutes and the presence of virions inside the droplet balance the evaporation chemical potential. The time needed to shrink the droplet to the final state can be approximated by

$$\tau_{ev}^{react} = \frac{R_0}{\alpha^{react}(1-RH)} \quad (D5)$$

For an initial radius of $R_0=100\text{nm}$, which is the upper limit where the stagnant reaction-limited evaporation regime is valid, the evaporation time is $\tau_{ev}^{react} = 16 \mu s / (1 - RH)$. Thus, in completely dry air with $RH=0$ the evaporation of a droplet with an initial radius of $R_0=100\text{nm}$ takes $16 \mu s$. This time is completely negligible compared to the floating time of a droplet with a radius of 100 nm , which is 20 days. In fact, evaporation cooling effects can be neglected in the reaction-rate-limited regime, since the heat transport stays diffusion limited and thus is faster than the reaction-limited diffusive transport of water molecules.

Appendix E: Convection effects on evaporation for laminar flow

To estimate air convection effects on the evaporation rate at an analytically manageable level, the concept of a concentration boundary layer will be used. In this section laminar flow will be assumed, finite-Reynolds number effects will be considered in subsequent appendices. In order to obtain the concentration boundary layer thickness, it is necessary to calculate the time it takes for a water molecule to diffuse a certain distance away from the droplet surface. The water diffusion velocity is given by

$$u(r) = \frac{dr(t)}{dt} = \frac{j(r)}{c(r)} = \frac{-D_w dc(r)/dr}{c(r)} = \frac{-D_w b/r^2}{1 + \frac{b}{r} \frac{b}{R+\Delta}} \quad (E1)$$

In the last step the presence of a concentration boundary layer at a radius $r=R+\Delta$ was assumed, where the concentration boundary layer width is defined by Δ and the stationary density distribution is given by

$$c(r) = c_0 \left(1 + \frac{b}{r} - \frac{b}{R+\Delta} \right) \quad (E2)$$

By this construction, at a radius $r=R+\Delta$, the water vapor concentration is equal to the ambient water vapor concentration c_0 . Using again the reactive boundary condition at the sphere surface $r=R$, Eq. (B3), the coefficient b is given by

$$b = R^2 k_c \frac{c_g/c_0 - 1}{D_w + k_c \Delta R / (R+\Delta)} \cong R^2 k_c \frac{c_g/c_0 - 1}{D_w + k_c \Delta} \quad , \quad (E3)$$

where $k_e c_l = k_c c_g$ was used. One sees that for a concentration boundary layer larger than the droplet radius, i.e. for $\Delta > R$, the effect of Δ disappears. In the last step therefore the opposite limit, $\Delta < R$, was considered. The total water evaporation flux J follows as

$$J = 4\pi R^2 j = 4\pi D_w c_0 b = 4\pi R^2 D_w k_c c_g \frac{1-RH}{D_w + k_c \Delta} \quad (E4)$$

The differential equation implied by Eq. (E1) is easily solved and gives

$$(r^3(t) - R^3) \left(1 - \frac{b}{R+\Delta}\right) / 3 + b(r^2(t) - R^2) / 2 = D_w b t . \quad (\text{E5})$$

Using $r=R+\Delta$ and $\Delta < R$, this simplifies to

$$D_w b \tau_{diff} \approx \Delta R^2 \left(1 - \frac{b}{R+\Delta}\right) + b \Delta R \approx \Delta R^2 + b \Delta^2 , \quad (\text{E6})$$

which defines the time it takes a water molecule to diffuse through the concentration boundary layer, which is called the diffusion time τ_{diff} . Inserting the diffusion-limited approximation for b from Eq. (E3), valid for $k_c \Delta > D_w$, the diffusion time becomes

$$\tau_{diff} = \frac{\Delta^2}{D_w(1-RH)} . \quad (\text{E7})$$

This diffusion time has to be compared with the convection time scale

$$\tau_{conv} = \frac{\pi r / 2}{v_{air}(r)} \approx \frac{\pi R^2}{2V\Delta} , \quad (\text{E8})$$

which is the time the flow needs to travel a quarter circle around the droplet at the boundary layer located at a radius of $r=R+\Delta$ from the droplet center. In Eq. (E8) the air flow profile around the droplet for laminar flow conditions has been used, given approximately by $v_{air}(r) \approx V \frac{r-R}{r} \approx V \Delta / R$, where V is the stationary droplet velocity from Eq. (A1b). By equating the diffusion and convection time scales τ_{diff} and τ_{conv} the concentration boundary layer thickness results as

$$\Delta = \Delta_0 (1 - RH)^{1/3} \quad (\text{E9})$$

with

$$\Delta_0 = \left(\frac{9 \pi \eta D_w}{4 \rho g} \right)^{1/3} = 80 \mu m . \quad (\text{E10})$$

Interestingly, the concentration boundary layer thickness does not depend on the speed with which the droplet falls to the ground, i.e., it does not depend on the droplet radius R . This result means that for radii larger than $R=80 \mu m$ and for dry air, one has $\Delta/R < 1$ and thus convection cannot be neglected and will accelerate evaporation. The diffusion-limited rate scenario is defined by $k_c \Delta > D_w$, which using Eqs. (B6) and (E9), is satisfied for relative humidity $RH < 1 \cdot 10^{-9}$, which is certainly always true. It transpires that convective evaporation in the laminar flow regime is basically always diffusion limited. Thus, the term proportional to D_w in the denominator of Eq. (E4) can be safely neglected and the diffusion-limited flux is obtained

$$J = 4\pi R^2 D_w c_g (1 - RH) / \Delta . \quad (\text{E11})$$

Mass conservation of the droplet can be written in terms of the droplet volume as

$$\frac{d}{dt} \left(\frac{4\pi}{3} R^3(t) \right) = -v_w J = -4\pi R^2 D_w c_g v_w (1 - RH) / \Delta \quad . \quad (E12)$$

The differential equation (E12) is easily solved with the result

$$R(t) = R_0 \left(1 - t \frac{D_w c_g v_w (1 - RH)^{2/3}}{\Delta_0 R_0} \right) = R_0 \left(1 - \alpha^{conv} t (1 - RH)^{2/3} / R_0 \right) \quad , \quad (E13)$$

where R_0 is the initial droplet radius and the numerical factor is given by

$$\alpha^{conv} = D_w c_g v_w / \Delta_0 = 7.9 \times 10^{-6} m/s \quad (E14)$$

and has units of a velocity. It is seen that shrinking of the radius is linear in time. Again, the evaporation time to a radius where osmotic effects due to dissolved solutes and the presence of virions inside the droplet balance the evaporation chemical potential can thus be approximated by the time needed to shrink the droplet radius down to zero, given by

$$\tau_{ev}^{conv} = \frac{R_0}{\alpha^{conv} (1 - RH)^{2/3}} \quad . \quad (E15)$$

Thus, at a relative humidity of $RH=0.5$, a droplet with an initial radius of $R_0=1$ mm has an evaporation time of $\tau_{ev}^{conv} = 200$ s, but needs (neglecting the shrinking of the radius) $\tau_a=0.017$ s to fall to the ground from a height of 2 meters, so it will not dry out before being absorbing at the ground. To accurately calculate the critical initial radius below which a droplet completely dries out before falling to the ground, Eq. (1) is rewritten in terms of the instantaneous droplet velocity and combined with Eq. (E13) to give

$$v(t) = \frac{D_R g m(t)}{k_B T} = \frac{R^2(t)}{\varphi} = \frac{R_0^2}{\varphi} \left(1 - \alpha^{conv} t (1 - RH)^{2/3} / R_0 \right)^2 \quad . \quad (E16)$$

The distance by which the droplet falls during its evaporation time, τ_{ev}^{conv} , follows by integration as

$$\Delta z = \int_0^{\tau_{ev}^{conv}} v(t) dt = \frac{R_0^3}{3\alpha\varphi(1-RH)^{2/3}} \quad . \quad (E17)$$

Now equating the distance Δz with the height z_0 , the critical droplet radius is

$$R^{crit} = \left(3\alpha\varphi^{conv} z_0 (1 - RH)^{2/3} \right)^{1/3} \quad , \quad (E18)$$

which for an initial height of $z_0=2$ m and for $RH=0.5$ gives $R^{crit}=67$ μ m. This is about the same radius where convection effects are relevant from Eq. (E9). Thus, convective evaporation effects do not play a significant role for droplets that are released from a height of $z_0 = 2$ m. For an initial height of $z_0=2$ km it follows from Eq. (E18) that droplets with a radius smaller than 670 μ m evaporate before they fall to the ground.

The results derived in this section neglect effects due to non-linear hydrodynamics, finite Reynolds number effects will be discussed in the following appendices. Evaporation cooling effects have not been treated explicitly in this appendix, but can be approximately accounted for multiplying the water vapor density c_g in Eq. (E14) by the correction term $\left(1 - \frac{\varepsilon_C \varepsilon_T}{1 + \varepsilon_C \varepsilon_T}\right)$ derived in Appendix C.

Appendix F: Non-laminar flow effects and flow boundary layer

Within the laminar flow boundary layer around an object, viscosity is relevant and laminar Stokes flow develops, outside this flow boundary layer potential flow is obtained. The flow boundary layer thickness scales like (26)

$$\delta = \left(\frac{\nu x}{V}\right)^{1/2} \quad (F1)$$

as a function of the distance x the flow has moved along the object, where V is the velocity of the object and $\nu = \eta/\rho_{air}$ is the kinematic viscosity. The density of air is denoted as ρ_{air} and given in Table I. The kinematic viscosity has units of a diffusion constant and characterizes the diffusivity of momentum or vorticity, its value in air is $\nu = 1.5 \times 10^{-5} \text{ m}^2/\text{s}$ and thus it is half the value of the water diffusion constant in air. This shows that momentum diffuses slightly slower than water in air, thus the flow boundary layer δ is expected to be smaller than the concentration boundary layer Δ . As result, flow boundary layer effects are expected to be relevant.

A simple estimate of the importance of momentum diffusion for a droplet moving in air is obtained by asking whether the flow boundary layer thickness δ is smaller than the droplet radius R for a flow that has travelled by a distance that corresponds to a quarter circle $x = \pi R/2$ around the droplet, i.e.

$$\delta = \left(\frac{\nu \pi R/2}{V}\right)^{1/2} < R \quad , \quad (F2)$$

which can be rewritten as

$$Re/\pi \equiv \frac{2RV}{\pi\nu} = \frac{2RV\rho_{air}}{\pi\eta} = \left(\frac{R}{R_*}\right)^3 > 1 \quad (F3)$$

and is equivalent to the condition that the Reynolds number Re is larger than π . The characteristic radius is defined as

$$R_* = \left(\frac{9\pi\eta^2}{4g\rho_{air}\rho R^3}\right)^{1/3} = 59\mu\text{m} \quad . \quad (F4)$$

The radius at which the Reynolds number becomes larger than π is therefore given by $R_* = 59\mu\text{m}$ and the flow around the sphere will not be laminar anymore. The typical momentum boundary layer thickness given in Eq. (F2) can be rewritten in terms of the characteristic radius as

$$\delta = \left(\frac{R_*^3}{R}\right)^{1/2} \quad , \quad (F5)$$

and is for a sphere with the characteristic radius given by R_* itself. Since R_* is for not too humid air smaller than the concentration boundary layer width $\Delta_0 = 80 \mu m$ from Eq. (E10), it follows that convection effects are modified in the presence of a flow boundary layer, which will be treated in Appendices G and H.

Appendix G: Convection effects on evaporation: Double boundary layer scenario in humid air

In this section the double boundary-layer problem will be addressed, where both concentration and fluid flow boundary layers with widths Δ and δ are present. It will be assumed that $\Delta < \delta$, which a posteriori will be shown to correspond to humid air; the opposite case $\Delta > \delta$ for dry air will be treated in Appendix H.

Due to the presence of the flow boundary layer, the air flow field around the droplet is compressed by a factor R/δ and approximately given by

$$v_{air}(r) \approx V \frac{R}{\delta} \left(\frac{r-R}{r} \right) . \quad (G1)$$

The convection time scale is defined as the time the flow needs to travel a quarter circle around the droplet at the concentration boundary layer located at a radius of $r=R+\Delta$ from the droplet center and is given by

$$\tau_{conv} = \frac{\pi r/2}{v_{air}(r)} \approx \frac{\pi R \delta}{2V \Delta} , \quad (G2)$$

which is smaller than the result for laminar flow in Eq. (E8) by a factor of δ/R . By equating the diffusion time scale τ_{diff} in Eq. (E7), which is not modified by flow boundary-layer effects, with the convection time scale τ_{conv} in Eq. (G2), the boundary layer thickness is

$$\Delta = \Delta_0 (1 - RH)^{1/3} \left(\frac{R_*}{R} \right)^{1/2} , \quad (G3)$$

where $\Delta_0 = 80 \mu m$ is the laminar concentration boundary layer width from Eq. (E10) and $R_* = 59 \mu m$ is the characteristic radius for non-laminar flow effects from Eq. (F4). To check whether the assumption $\Delta < \delta$ used in this Appendix is satisfied, Eq. (G3) is divided by the momentum boundary layer width δ from Eq. (F5) to obtain

$$\frac{\Delta}{\delta} = (1 - RH)^{1/3} \frac{\Delta_0}{R_*} . \quad (G4)$$

It transpires that the assumption $\Delta < \delta$ is satisfied for humid air with a relative humidity larger than

$$RH > 1 - \left(\frac{\Delta_0}{R_*} \right)^{-3} = 0.58 . \quad (G5)$$

When is the double-boundary-layer evaporation regime entered? This question is equivalent to asking when the boundary layer width Δ as given by Eq. (G3) becomes smaller than the radius R . For an intermediate humidity that coincides with the threshold value Eq. (G5), it is

found that the double-boundary-layer evaporation regime is entered for radii $R > R_* = 59\mu\text{m}$, i.e., as soon as boundary flow effects occur. For more humid the threshold radius increases and follows from Eq. (G3).

The diffusion-limited rate scenario is defined by $k_c\Delta > D_w$, which using Eqs. (B6) and (G3), is satisfied for radii

$$R < (1 - RH)^{2/3} \left(\frac{\Delta_0^2 R_*}{(D_w/k_c)^2} \right) = (1 - RH)^{2/3} 38 \text{ m} . \quad (\text{G6})$$

It transpires that double-boundary layer convective evaporation in humid air is always diffusion limited. Thus, the differential equation Eq. (E12) valid in the diffusion limit can be used, which in conjunction with Eq. (G3) yields

$$R(t) = \left(R_0^{1/2} - t \frac{D_w c_g v_w (1 - RH)^{2/3}}{2\Delta_0 R_*^{1/2}} \right)^2 = \left(R_0^{1/2} - \alpha^{dbl1} t (1 - RH)^{2/3} \right)^2 , \quad (\text{G7})$$

where R_0 is the initial droplet radius and the numerical factor is given by

$$\alpha^{dbl1} = \frac{D_w c_g v_w}{2\Delta_0 R_*^{1/2}} = 5.7 \times 10^{-4} \text{ m}^{1/2} / \text{s} . \quad (\text{G8})$$

It is seen that the shrinking the radius slows down over time. Evaporation cooling effects have not been treated explicitly, but can be approximately accounted for multiplying the water vapor density by the correction term $\left(1 - \frac{\varepsilon_c \varepsilon_T}{1 + \varepsilon_c \varepsilon_T} \right)$ derived in Appendix C.

Appendix H: Convection effects on evaporation: Double boundary layer scenario in dry air

In this section, it will be assumed that the concentration boundary layer width is larger than the flow boundary layer width, i.e. $\Delta > \delta$, which a posteriori will be shown to correspond to dry air. The calculation closely follows Appendix G.

At the concentration boundary layer, since $\Delta > \delta$, the air flow field around the droplet is unperturbed by the presence of the droplet and given by $v_{air}(r) \approx V$. The convection time scale is therefore given by

$$\tau_{conv} = \frac{\pi r / 2}{v_{air}(r)} \approx \frac{\pi R}{2V} , \quad (\text{H1})$$

which is smaller than the corresponding result in Eq. (G2). By equating the diffusion time scale τ_{diff} in Eq. (E7), which is not modified by flow boundary-layer effects, with the convection time scale τ_{conv} in Eq. (H1), the boundary layer thickness results as

$$\Delta = (1 - RH)^{1/2} \left(\frac{\Delta_0^3}{R} \right)^{1/2} , \quad (\text{H2})$$

where $\Delta_0 = 80 \mu m$ is the laminar concentration boundary layer width from Eq. (E10). To check when the assumption $\Delta > \delta$ used here is satisfied, Eq. (H2) is divided by the momentum boundary layer width δ from Eq. (F5) to obtain

$$\frac{\Delta}{\delta} = (1 - RH)^{1/2} \left(\frac{\Delta_0}{R_*} \right)^{3/2} . \quad (H3)$$

It transpires that the assumption $\Delta > \delta$ is satisfied for dry air with a relative humidity smaller than

$$RH < 1 - \left(\frac{\Delta_0}{R_*} \right)^{-3} = 0.58 . \quad (H4)$$

When is the double-boundary-layer evaporation regime entered? This question is equivalent to asking when the boundary layer width Δ as given by Eq. (H2) becomes smaller than the radius R . For an intermediate humidity that coincides with the threshold value Eq. (H4), it follows that the double-boundary-layer evaporation regime is entered for radii $R > R_* = 59 \mu m$, i.e., as soon as boundary flow effects according to Eq. (F4) occur.

The diffusion-limited rate scenario is defined by $k_c \Delta > D_w$, which using Eqs. (B6) and (H2), is satisfied for radii

$$R < (1 - RH) \left(\frac{\Delta_0^3}{(D_w/k_c)^2} \right) = (1 - RH) 51 m . \quad (H5)$$

It transpires that double-boundary layer convective evaporation in dry air is always diffusion limited. Thus, the differential equation Eq. (E12) can be used, which in conjunction with Eq. (H2) yields

$$R(t) = \left(R_0^{1/2} - t \frac{D_w c_g v_w (1 - RH)^{1/2}}{2 \Delta_0^{3/2}} \right)^2 = \left(R_0^{1/2} - \alpha^{dbl2} t (1 - RH)^{1/2} \right)^2 , \quad (H6)$$

where R_0 is the initial droplet radius and the numerical factor is given by

$$\alpha^{dbl2} = \frac{D_w c_g v_w}{2 \Delta_0^{3/2}} = 3.5 \times 10^{-4} m^{1/2} / s . \quad (H7)$$

Evaporation cooling effects have not been treated explicitly, but can be approximately accounted for by multiplying the water vapor density c_g by the correction term $\left(1 - \frac{\epsilon_C \epsilon_T}{1 + \epsilon_C \epsilon_T} \right)$ derived in Appendix C.

Appendix I: Falling speed for large Reynold numbers

The Stokes approximation used for calculating the stationary falling speed of droplets in Eq. (A1b) is a low-Reynolds number approximation. An empirical formula for the settling speed of a sphere in air, that is valid over the entire range of Reynold numbers, is

$$V = \sqrt{\frac{8gR\rho}{3\rho_{air}c_D}} , \quad (I1)$$

where the resistance coefficient is given by

$$c_D = \frac{24}{Re} + \frac{4}{Re^{1/2}} + 0.4 \quad (I2)$$

and the Reynolds number Re is defined in Eq. (F3). The result of Eq. (A1b) is reproduced by Eq. (I1) when only the first term in Eq. (I2) is used. The accuracy of this low-Reynolds number approximation can be checked by comparing the first and third terms in Eq. (I2), which become equal for a Reynolds number of about $Re=60$, which corresponds, using again Eq. (F3), to a radius of about $(\frac{60}{\pi})^{1/3} R_* = 157 \mu\text{m}$. This suggests that the falling speed according to Eq. (A1b) is quite accurate for radii below $157 \mu\text{m}$. For larger radii the falling speed will be reduced and thus the absorption time will be increased. Therefore, the absorption times presented in this note are lower estimates for radii larger than about $157 \mu\text{m}$.

Appendix J: Internal mixing effects

The calculations so far assume that diffusion inside the droplet is sufficiently rapid, so that the water concentration at the droplet surface does not differ significantly from the mean water concentration in the droplet. It will turn out that this is a limiting factor for the maximal droplet size that can evaporate at the speed predicted here. According to the diffusion law, the time it takes for a water molecule to diffuse over the droplet radius R inside the droplet is

$$\tau_{mix} = \frac{R^2}{2D_w^l} \quad , \quad (J1)$$

where D_w^l is the molecular water self-diffusion constant in liquid water. The mixing time within a droplet of radius $R=10 \mu\text{m}$ is $\tau_{mix} = 25 \text{ms}$ and inside a droplet of radius $R=100 \mu\text{m}$ it is $\tau_{mix} = 2.5 \text{s}$. Equating τ_{mix} with the mean absorption time Eq. (1), the mixing time inside the droplet is only shorter than the absorption time for radii smaller than $100 \mu\text{m}$. For larger droplets the internal diffusion will slow down evaporation and droplets will fall to the ground without evaporation taking place to a sufficient degree. Convection effects inside the droplet, due to shear coupling to the air flow field, will counteract this effect, but are not considered here. Also, the increase of the internal droplet viscosity due to increasing solute concentration and the presence of a solid solute phase is not considered and will further slowdown the diffusion inside droplets.

Appendix K: Solute-induced vapor pressure reduction effects

Any solute present in the water droplet decreases the water vapor pressure. The colligative effect is basically due to the dilution of the liquid water and follows from the equilibrium equation for the vapor concentration

$$c_g = c_l e^{\mu_{ex}/k_B T} \quad , \quad (K1)$$

which depends exponentially on the water excess chemical potential, at room temperature given by $\mu_{ex} = -\frac{27 \text{kJ}}{\text{mol}}$. Assuming that initially the volume fraction of solutes is Φ_0 and the

initial radius is R_0 , the water concentration in the liquid droplet with reduced radius R follows as

$$c_l = \frac{1}{v_w} \left(1 - \Phi_0 \frac{R_0^3}{R^3} \right) . \quad (K2)$$

Inserting Eq. (K2) into Eq. (K1) one obtains for the water vapor concentration in the presence of solutes

$$c_g^{sol} = c_g \left(1 - \Phi_0 \frac{R_0^3}{R^3} \right) , \quad (K3)$$

which corresponds to the law of Raoult. Here, c_g represents the water vapor concentration in the absence of solutes. Non-ideal effects can be included via the excess chemical potential and are described by an activity coefficient different from unity, which is not pursued here. Rewriting Eq. (C12) slightly, one arrives at

$$J = 4\pi R D_w \left(1 - \frac{\varepsilon_C \varepsilon_T}{1 + \varepsilon_C \varepsilon_T} \right) (c_g^{sol} - c_0) . \quad (K4)$$

Together with Eq. (K3), one obtains the modified diffusive water flux in the presence of solutes as

$$J = 4\pi R D_w \left(1 - \frac{\varepsilon_C \varepsilon_T}{1 + \varepsilon_C \varepsilon_T} \right) \left(c_g \left(1 - \Phi_0 \frac{R_0^3}{R^3} \right) - c_0 \right) . \quad (K5)$$

The mass conservation equation follows as

$$\frac{d}{dt} \left(\frac{4\pi}{3} R^3(t) \right) = -v_w J = -2\pi R \theta \left(1 - \Phi_0 \frac{R_0^3}{R^3} - RH \right) , \quad (K6)$$

where θ is defined in Eq. (C14). Equation (K6) gives rise to the differential equation

$$\frac{2RdR}{1 - R_\infty^3/R^3} = -\theta(1 - RH)dt, \quad (K7)$$

where the equilibrium droplet radius that is obtained in the long-time limit is defined as

$$R_\infty = R_0 \left(\frac{\Phi_0}{1 - RH} \right)^{1/3} . \quad (K8)$$

The solution of this differential equation can be written as

$$t(R) = \frac{R_\infty^2}{\theta(1 - RH)} \left[\mathcal{L} \left(\frac{R_0}{R_\infty} \right) - \mathcal{L} \left(\frac{R}{R_\infty} \right) \right] , \quad (K9)$$

where the scaling function is given by

$$\mathcal{L}(x) = x^2 - \frac{2}{\sqrt{3}} \arctan \left(\frac{1 + \frac{2}{x}}{\sqrt{3}} \right) - \frac{1}{3} \ln \left(\frac{x^2 + x + 1}{(x - 1)^2} \right) . \quad (K10)$$

The scaling function exhibits the asymptotic behavior

$$\mathcal{L}(x) \cong x^2 \quad (\text{K11})$$

for large arguments and

$$\mathcal{L}(x) \cong +\frac{2}{3} \ln(1 - 1/x) \quad (\text{K12})$$

for small arguments $x \rightarrow 1$. A quite accurate crossover expression is produced by summing the two limits as

$$\mathcal{L}(x) \cong x^2 + \frac{2}{3} \ln(1 - 1/x) . \quad (\text{K13})$$

Appendix L: Surface tension effects

The large surface tension of water increases the vapor pressure produced by droplets. The surface free energy of a droplet is given by

$$F = 4\pi\gamma R^2 . \quad (\text{L1})$$

The chemical potential contribution, the so-called Kelvin potential, reads

$$\mu_{Kel} = \frac{dF}{dN} = \frac{dR}{dN} \frac{dF}{dR} = \frac{2\gamma v_w}{R} , \quad (\text{L2})$$

where the number of water molecules inside the droplet is taken as $N=4\pi R^3/(3v_w)$. Inserting numbers, the rescaled Kelvin potential reads

$$\frac{\mu_{Kel}}{k_B T} = \frac{10^{-9}m}{R} , \quad (\text{L3})$$

which is significant compared to the water excess chemical potential only for droplet radii smaller than one nanometer.

To avoid confusion: the Laplace pressure

$$P_{Lap} = -\frac{dF}{dV} = -\frac{dR}{dV} \frac{dF}{dR} = \frac{2\gamma}{R} \quad (\text{L4})$$

is significant and reaches 1 bar for a droplet radius of 1 μm , but is unrelated to the vapor pressure.